POLITECNICO DI TORINO
Repository ISTITUZIONALE

Rapid antibody-free fluorescence quenching-based protein detection using molecularly imprinted sensors

Original
Rapid antibody-free fluorescence quenching-based protein detection using molecularly imprinted sensors / Sinnona, F., Abdelgawad, M.S., Ono, S., Shen, A.Q., Sullivan, M.V.. - In: SENSORS AND ACTUATORS. B, CHEMICAL. - ISSN 0925-4005. - 461:(2026). [10.1016/j.snb.2026.139977]

Availability:
This version is available at: 11583/3016370 since: 2026-10-07T04:59:45Z

Publisher:
Elsevier

Published
DOI:10.1016/j.snb.2026.139977

Terms of use:

This article is made available under terms and conditions as specified in the corresponding bibliographic description in the repository

Publisher copyright

(Article begins on next page)

29 November 2026

Sensors & Actuators: B. Chemical 461 (2026) 139977



Contents lists available at ScienceDirect

Sensors and Actuators: B. Chemical

journal homepage: www.elsevier.com/locate/snb





Rapid antibody-free fluorescence quenching-based protein detection using molecularly imprinted sensors

Federico Sinnona [a], Mohamed S. Abdelgawad [b], Shun Ono [a], Amy Q. Shen [a,*], Mark V. Sullivan [a,*]

[a] Micro/Bo/Nanofluidics Unit, Okinawa Institute of Science and Technology Graduate University, 1919-1 Tancha, Onna-son, Okinawa 904-0495, Japan
[b] Complex Fluids and Flows Unit, Okinawa Institute of Science and Technology Graduate University, 1919-1 Tancha, Onna-son, Okinawa 904-0495, Japan

ARTICLE INFO

Keywords:
Molecularly Imprinted Polymer
Low-Cost
Protein Biomarker
Diagnostics
Fluorescent Quenching

ABSTRACT

A dual-function, fluorescence quenching-based chemical sensing platform for rapid protein detection is developed using hydrogel molecularly imprinted polymer (MIP) microparticles that serve as both synthetic recognition elements and direct optical transducers. MIPs were imprinted against bovine hemoglobin (BHb) and fluorescently labelled via incorporation of fluorescein O-methacrylate, enabling direct optical transduction upon target binding. Using bovine hemoglobin as a model target, the dual-function materials exhibited high affinity (K_D = 1.91 μM) and imprinting- and selectivity factor values (2.3 and 1.7, respectively), exceeding accepted performance thresholds. A central novelty of this work is the emphasis on operational sensor performance under dynamic environments, moving beyond static equilibrium metrics. Rheological and extensional-flow characterization revealed that the molecular imprinting process induces distinct mechanical reinforcement of the polymer network, providing enhanced resistance to deformation and a higher linearity limit compared to non-imprinted controls. The fluorescence quenching assay enabled rapid, mix-and-measure detection to BHb directly from human serum, achieving a limit of detection of 8.38 nM and a limit of quantification of 25.39 nM, with recovery rated of 97.5–100.7% and minimal analytical error. This work demonstrates a robust, and scalable fluorescence sensing strategy that offers a practical alternative to antibody-based assays for protein biomarker detection with microfluidic diagnostic platforms.

1. Introduction

Protein biomarkers are typically used as indicators to diagnose disease or monitor the activity of diseases and assess the therapeutic response [1–3]. This results in a growing need to further develop and understand better diagnostics, thus building platforms capable of detecting new disease and illness when they emerge. This typical involves the use of a recognition material, that will be able to specifically bind to a target molecule using non-covalent bonding, such as hydrogen bonding, metal coordination, hydrophobic forces, or van der Waals for of interaction [4,5]. Antibodies are natural molecular recognition entities that are well-used in medical diagnostics, because they have naturally evolved physiological interactions that achieve target selectivity and specificity [6–8]. When these entities are incorporated into an analytical methodology, they offer excellent sensitivity and selectivity, making their use a popular choice [9]. However, as with many biological-based systems, reproducibility is a potential issue due to batch-to-batch variations and processing stability. Furthermore, they can be expensive to produce, often with limited reusability and their performance is severely affected by changes in temperature and pH [6,10]. Stability of a recognition material is vital to any analytical performance that relies upon specificity and affinity; thus, antibody use can be compromised in a nonclinical/laboratory setting, especially when used by untrained professionals. While work has been achieved to increase stability within antibodies, particular for their use within lateral flow tests and low-cost biosensors that are needed to be deployed outside the laboratory, this has only alleviated the issue and not solved the degradation problem [6]. This has led to the search for synthetic recognition material as potential alternatives that can be used without the concern of degradation.

Molecularly imprinted polymers (MIPs) have emerged as promising synthetic alternatives to natural recognition materials [11,12]. MIPs can be produced inexpensively and reproducibly and exhibit excellent chemical and thermal stability, enabling operation under conditions

* Corresponding authors.
E-mail addresses: amy.shen@oist.jp (A.Q. Shen), mark.sullivan@oist.jp (M.V. Sullivan).

https://doi.org/10.1016/j.snb.2026.139977
Received 31 January 2026; Received in revised form 12 April 2026; Accepted 13 April 2026
Available online 16 April 2026
0925-4005/© 2026 The Author(s). Published by Elsevier B.V. This is an open access article under the CC BY license (http://creativecommons.org/licenses/by/4.0/).

that would denature antibodies. [13,14]. The imprinting of proteins is particularly attractive, as this offers the potential for non-biomolecular recognition, thus potentially overcoming the possible issues that come with using biological-based recognition materials (immunoresponse, enzymatic degradation, denaturation) [15,16]. While, molecular imprinting appears to offer the ideal solution to these issues, it is not without its own challenges, whereby monomer, crosslinker and solvent choice become important factors. This is to prevent any potential template protein precipitation or unravelling of the tertiary or quaternary conformations of the template protein, which negatively impacts the binding site formation within the MIP, thus resulting in the production of low affinity MIPs [16,17]. The development of hydrogel-based MIPs offers some reprieve in the challenges of protein-imprinting, with the high-water compatibility providing protein stability during the MIP formation [18,19]. Utilizing a one-pot synthesis methodology produces hydrogel-based MIPs in their simplest form, with the template, monomers, crosslinker, initiator are dissolved in an aqueous solution and reacted together at ambient template. This produces a bulk monolith that is then processed into smaller microparticles allowing for access and subsequent removal of the template molecule. Whilst this post-processing can be destructive and potentially affect the affinity of the MIP, this method still provides extremely high yields of useable material that offer excellent affinity towards the target [20].

Whilst MIPs have typically found their niche within diagnostic platforms [21], with one such application is to utilize the affinity properties of MIPs within a fluorescent-based assay [22,23]. Fluorescence assays are commonly used with protein biomarker diagnostics, and work by measuring the emission intensity generated by a sample, which is proportional to the concentration of the fluorophore present. Typically, fluorescence-type assays use an antibody that has been labelled with a fluorophore [24,25], but as MIPs can be rationally designed, fluorophores can easily be incorporated as demonstrated by Li et al. [26] This simplicity of design reduces the need for the more complicated sandwich style assays and offers fluorescent quenching as an option, whereby the fluorescence intensity of a sample can be measurably decreased due the binding of the target molecule. Takeuchi et al. investigated this process, by using the photoluminescence properties of a porphyrin molecule incorporated into the MIP polymer structure and used fluorescent quenching to investigate and display the binding phenomena of the MIP [27]. The use of fluorescence and subsequent quenching can offer significant advantages within sensing, due to its high sensitivity, simplicity, and diversity [28]. Furthermore, with the right choice of fluorophore, low limits of detection are easily achieved with detection of protein biomarkers, direct from complex media samples, without the need for sample preparation.

Recent advances in fluorescence-based molecularly imprinted polymer (MIP) sensors have demonstrated the feasibility of incorporating fluorophores into imprinted matrices and enabling protein detection in complex media; however, these systems are predominately based on surface-confined architectures such as nanoMIPs, thin films, or core-shell structures, often requiring multistep fabrication, template immobilisation, or secondary labelling and signal amplification strategies to generate measurable responses [29,30]. In contrast, this work adopts a fundamentally different approach by employing bulk hydrogel imprinting to produce gram-scale quantities of microparticulate MIPs that function simultaneously as recognition elements and optical transducers, The intrinsic incorporation of a fluorescent monomer within the polymer network enables a direct, reagent-free fluorescence quenching mechanism upon target binding, eliminating the need for immobilisation, washing, or amplification steps commonly required in conventional assays [31]. Furthermore, whilst most fluorescence-based MIP sensors are evaluated under static, equilibrium conditions, relatively limited attention has been given to their behaviour under flow, despite the importance of dynamic environments in microfluidic and continuous sensing applications [32]. Here we address this gap by demonstrating that molecular imprinting not only imparts chemical selectivity but also mechanistically reinforces the hydrogel network, enabling stable binding and optical response under extensional flow conditions. Collectively this integration of scalable fabrication, intrinsic signal transduction, and validation under dynamic conditions establishes a distinct and practically relevant sensing paradigm beyond existing fluorescence-based MIP systems.

Here, we report a fluorescence-based chemical sensing platform for rapid, antibody-free protein detection using hydrogel molecularly imprinted polymer (MIP) microparticles as synthetic recognition elements. Target binding within imprinted cavities induces intrinsic fluorescence quenching, enabling direct optical transduction in a simple mix-and-measure format without surface immobilisation, washing steps, or signal amplification. Beyond molecular recognition, this study emphasis operational sensor performance, demonstrated through quantitative detection of hemoglobin directly from untreated human serum with nanomolar sensitivity, signal robustness, and functionality under flow conditions relevant to microfluidic and flow-through architectures. Hemoglobin was selected as a representative model protein rather than a disease-specific biomarker; as a large multimeric, and structurally complex target, it presents a stringent test of imprint fidelity, binding accessibility, and matrix tolerance [33,34], and successful detection therefore indicates the platform's broader capacity to recognise proteins of comparable size and complexity including clinically relevant biomarkers such as ferritin, C-reactive protein, and inflammatory cytokines [35]. Bovine hemoglobin (BHb) was selected as a model target due to its structural complexity and relevance as a representative globular protein, rather than as a clinically specific biomarker. With a molecular weight of ~64.5 kDa and a multimeric quaternary structure, hemoglobin presents a stringent test for molecular imprinting, requiring the formation of binding sites capable of accommodating large, conformationally complex targets [20]. Importantly, molecular imprinting is inherently a template-driven and transferable strategy, whereby the same polymerisation approach can be readily adapted to clinically relevant biomarkers (e.g., C-reactive protein, cardiac troponin, or cytokines) by substitution of the template during synthesis, with comparable performance reported across a range of protein targets [35,36]. Furthermore, successful detection in untreated human serum demonstrates that the sensing platform can operate in complex biological matrices, supporting its broader applicability to clinically relevant analytes. In this context, BHb serves as a rigorous proof-of-concept target for establishing a generalisable sensing framework. In contrast to conventional MIP-based fluorescence sensors and beyond traditional affinity measurements, sensor performance was further validated under flow using an optimised shape ross-slot extensional rheometer (OSCER), which functions as a mechanical stress test by exposing sensors to stagnation-point flows that emulate demanding microfluidic environments; imprinting was shown to mechanically reinforce the hydrogel network, preserving optical stability under deformation. Our work introduces three key advances (i) gram-scale, low-cost fabrication of hydrogel MIP microparticles compared with nanoMIP or thin-film approaches; (ii) intrinsic fluorescent labelling of the imprinted matrix enabling reagent-free quenching readout upon target binding; and (iii) systematic evaluation of mechanical and binding stability under extensional flow. These features establish a practical, scalable, and operationally robust sensing architecture for antibody-free protein detection in complex biological media.

2. Materials and methodology

2.1. Materials

Ammonium persulfate (APS), Bovine Hemoglobin (BHb), Bovine Serum Albumin (BSA), fluorescein *O*-methacrylate, glacial acetic acid (AcOH), *N*-(hydroxymethyl)acrylamide (NHMAm), *N,N'*-methylenebis (acrylamide) (mBAm), sodium dodecyl sulfate (SDS), and tetramethylethyldiamide (TEMED), were all purchased and used without

purification from Sigma-Aldrich, Tokyo, Japan.

Scanning electron microscopy (SEM) analysis was performed using a JSM-7900F 8530FA from JEOL Co., Japan.

3. Methodology

3.1. Molecularly imprinted polymer (MIP) preparation

Using an adapted methodology, molecularly imprinted hydrogel microparticles were produced using a 10% crosslinking density of monomer to crosslinker (9:1) ratio, which was found to produce an optimum flexible material to enable specific protein binding [20,37].

Into an Eppendorf tube, 12 mg of target protein (BHb) was dissolved into 970 μL of MilliQ water then vortexed for 1 min. Next, 0.76 mmol of the functional monomer NHMAm was added, vortexed for 1 min and allowed to self-assemble around the surface of template to form an optimal monomer-template complex. Following this, the crosslinker mBAm was added at a ratio of 9:1 by weight, and the mixture was further vortexed for 1 min, before the addition of 10 μL 5% TEMED (v/v) solution and 20 μL 5% APS (w/v) solution. This mixture was vortex for 1 min, before being purged with nitrogen for 5 min and full polymerization occurring overnight at room temperature (approximately 20 °C). A corresponding non-imprinted polymer (NIP), used as a control, was produced using the same protocol, but in the absence of the protein template.

After polymerization the bulk hydrogels were granulated separately using a 53-micron sieve, producing microparticles, that were then washed with 1 mL of a 10% (w/v): 10% (v/v) SDS:AcOH solution, twice. This allows for the denaturation and subsequent removal of the template protein from the recognition cavities contained within the MIP. The gels were then washed with 1 mL volumes of MilliQ water, until all SDS:AcOH solution was removed (minimum five washes). It is imperative that all SDS:AcOH solution is removed from the gel before rebinding can occur as any leftover residue could significantly impact the binding performance of the MIPs. The corresponding control polymers (NIPs) were also processed in the same manner.

Throughout this work, "MIP" and "NIP" refer to chemically identical hydrogel networks synthesised under identical conditions, differing only in the presence or absence of the template protein during polymerisation.

3.2. Microfluidic platforms for shear flow

An optimised shape cross-slot rheometer (OSCER) device was produced using an ELEGOO Mars 5 Ultra. The OSCER is based on a planar cross-slot geometry with two incoming and outgoing flows placed orthogonal to each other, as described by Calabrese at al. [38] The device has a height $H = 0.3$ mm and a channel width of $W = 0.3$ mm at the inlets and outlets, yielding an aspect ratio $\alpha = H/W = 1$, generating a good approximation of 2D flow field, which is extensional-dominated and shear-free in a large region around the stagnation point [38]. The flow inside the channels is generated by Nemesys low-pressure syringe pumps (Centoni, GmbH) and Hamilton Gastight syringes, which infuse the liquid at the inlet. The flows were equilibrated for at least 5 s before injection of the MIP microparticles and measurements and confirmed as being steady by inspection of the microparticle image. All measurements were performed at ambient temperature (25 ± 1 °C).

3.3. Molecularly imprinted polymer performance and kinetic studies

The binding performance of the condition MIPs and corresponding NIPs was investigated and characterized using a Nanodrop 2000c UV/Visible spectrometer, whereby 20 mg of the hydrogel was treated with 60 μL of a target protein (BHb) solution between the concentrations of 0–1 mg mL^{-1}. The polymer-protein mixture was vortexed for 1 min, then left for 5 min to allow for the protein target molecule to associate with the polymer, at room temperature (approximately 20 °C). the hydrogels were then centrifuged for 5 min, and the supernatant was collected and analysed by UV/Vis (at 405 nm). The Selectivity of the MIP/NIP microparticles was further investigated through the non-specific binding of a non-target protein (BSA), with the supernatant analysed at 220 nm.

3.4. Rheological characterization

Rheological measurements for both MIP (target loaded) and NIP (target loaded) hydrogels were performed using an Anton Paar MCR 502 rotational rheometer, equipped with a 21 mm diameter cone and plate geometry (1° cone angle). A sandblasted bottom plate was used to minimize the slip effect. The temperature was maintained at a constant 25 °C throughout the measurements using a Peltier bottom plate. For effective evaporation, humidity, and uniform temperature distribution control, a solvent well filled with water was used together with a solvent trap, covering the sample throughout the measurement process.

The MIP/NIP hydrogel sample was loaded into the rheometer and heated to 25 °C for 5 min to reach thermal equilibrium. A strain amplitude sweep test is performed by applying an oscillatory shear at a fixed angular frequency of 1 rad/s, increasing the strain amplitude logarithmically from 0.01% to 100%. Next, the hydrogels (MIP/NIP) were subjected to oscillatory three-step thixotropy test, the hydrogel was subjected to different strain amplitudes that were within and outside the linear viscoelastic region. The test sequence involved an initial strain amplitude of 0.1% for 1 min, followed by a high strain amplitude of 100% for 1 min. After this, the hydrogel was allowed to recover at a strain amplitude of 0.1% for 10 min. Each test was repeated three times to establish repeatability of the measurements.

3.5. Molecularly imprinted polymer fluorescent quenching assay

A MIP-based competitive assay was designed for the detection of the protein hemoglobin (BHb). The assay uses a fluorescently labelled MIP (F-MIP), prepared using the same methodology but with the addition of fluorescein *O*-methacrylate (2.5 pmol) into the prepolymerisation mixture.

Development and calibration of the assay consisted of solutions of known concentrations (0–45 nM) of BHb were prepared in 450 μL of MilliQ water, followed by the addition of 20 mg of F-MIP/NIP to the sample. This was the vortexed for 30 s and left for 5 min to allow the protein to associate with the imprinted or non-imprinted gel. The protein-F-MIP/NIP solutions were analysed using a Qubit® 3.0 fluorometer with an excitation at 470 nm and an emission scan range of 510–580 nm. A calibration curve was created by plotting the amount of protein loaded (mg mL^{-1}) versus intensity (CPS). The calibration was repeated, but with the target protein spiked Human Serum, instead of MilliQ water.

To test the validity of the assay 450 μL samples of human serum were spiked with known concentrations (0.5, 0.9 and 1.5 mg mL^{-1}). Next, 20 mg of F-MIP/NIP was added to the sample and vortexed for 30 s and left for 5 min to allow the protein to associate with the gel. The solutions were then analysed using a Qubit® 3.0 fluorometer with an excitation at 470 nm and an emission scan range of 510–580 nm. The measurements were then compared with the calibration plot to evaluate the error within the assay.

4. Results and discussion

Molecularly imprinted polymers (MIPs) and fluorescently labelled MIPs (F-MIPs), and their corresponding non-imprinted polymers (NIPs), were successfully synthesised, using NHMAm as the functional monomer, mBAm as the crosslinker, fluoresceine *O*-methacrylate as the fluorescent label (F-MIP/NIP only) and water as the polymerisation solvent. Traditionally, organic solvents were typically used within the production of MIPs, but these have been shown to readily denature

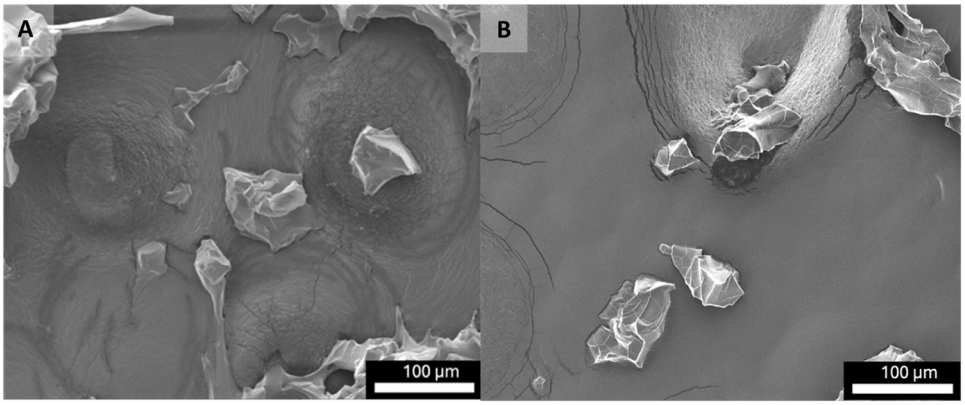

Fig. 1. SEM images of the MIP microparticles (A) and NIP microparticles (B).

Table 1
Percentage of BHb target protein and BSA non-target protein binding to the different hydrogel microparticles. N = 3.

	Percentage of Protein Binding (%)	
Polymer	**BHb**	**BSA**
MIP	89.4 (± 0.8)	45.5 (± 4.6)
NIP	41.9 (± 1.7)	47.1 (± 3.0)
F-MIP	83.7 (± 2.9)	50.0 (± 6.1)
F-NIP	35.9 (± 0.7)	50.0 (± 3.8)

proteins, making the unsuitable for use with this investigation. Acrylamide-based monomers have shown they offer excellent functionality and water-solubility, important factors to consider when imprinting protein targets. NHMAm has been previously shown to offer excellent potential as a functional monomer in the production of hydrogel-based MIPs, thus is an ideal choice to produce the imprinted microparticles produced in this study [20,39].

The hydrogels were produced as a bulk monolith (1 g), that after post-polymerisation processing, produced microparticles at an approximate 70%, with approximate 0.7 g of usable materials. The protein (BHb) template was removed from the MIP cavities using as series of SDS:AcOH washes, whereby the solution efficiently removes the protein through denaturisation of the protein, altering the shape and structure of the template [39]. This leads to the destruction of the electrostatic forces of the MIP-Protein complexation, with subsequent washed used to completely remove the protein from the MIP, leaving behind the MIP particles, with free cavities that are specific to the chosen temple. Scanning electron microscopy (SEM) was used to determine the size and morphology of the microparticles, with the images shown in Fig. 1.

As Fig. 1 shows, the post-polymerization process that involves a grinding and sieving of the bulk hydrogel monolith, produces irregular shaped particles, of approximately 20 — 70 µm. This irregularity is to be expected and is an artifact of the post-polymerization processing and leads to a heterogenous mixture of particles, which could potentially affect the binding properties of the imprinted materials.

4.1. Rebinding experiments

The rebinding of the target protein (BHb) on the MIP microparticles is presented in Table 1 and Fig. 2 and clearly shows that MIP and F-MIP microparticles perform the best with an 89.4% and 83.7% rebinding of the target protein. There is a slight difference between the binding performance between the MIP and F-MIP, which can be considered minor, thus showing that the inclusion of the fluorescent label does not impact the performance of the MIP. While, the control non-imprinted polymers (NIP and F-NIP), also presented in Table 1 and Fig. 2, still showed some degree of binding the target protein, with 41.9% and 35.9% binding of the target protein, these values are significantly less than the values for the MIPs. The decrease in binding is to be expected and is due to the formation of specific binding cavities during the imprinting process, while the control polymers (NIPs/F-NIP) are still

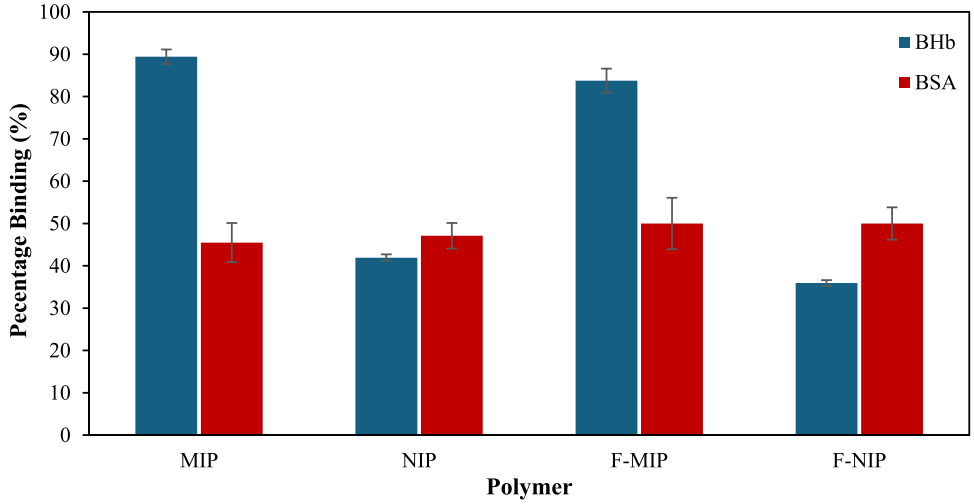

Fig. 2. Percentage binding of the target protein BHb (blue) and the non-target protein BSA (red) to the different MIPs and their corresponding NIPs. Data represent mean ± SD (n = 3).

Table 2
Imprinting Factor (IF) values and Selectivity Factor (SF) values for the different hydrogel MIPs and their corresponding NIPs.

Polymer	IF-BHb (MIP/NIP)	IF-BSA (MIP/NIP)	SF-MIP (BHb/BSA)	SF-NIP (BHb/BSA)
MIP	2.13	0.96	1.96	0.88
F-MIP	2.33	1.00	1.67	0.71

expected to show some degree of non-selective binding because of the functional monomer (NHMAm) used within the production of hydrogels.

The binding specificity of imprinted materials (MIP/F-MIP) was evaluated further, through the binding of a non-target protein (BSA) to the MIPs (and corresponding NIPs). BSA was chosen due to similarities in size, molecular weight and solvent accessible surface area (SASA), resulting in the ideal opportunity to show specificity of the materials [40]. Bovine serum albumin (BSA) was selected as a representative competing protein due to its widespread use as a stringent benchmark for evaluating non-specific binding in molecularly imprinted polymer systems. As one of the most abundant proteins in biological fluids, BSA possesses a comparable molecular weight (~66 kDa), globular structure, and high solvent-accessible surface area, making it particularly prone to non-specific adsorption within hydrogel networks [36,41]. Consequently, successful discrimination against BSA is widely regarded as a conservative indicator of MIP specificity, as it challenges both shape-selective recognition and suppression of non-specific physiochemical interactions. Moreover, recent studies have shown that BSA often represents a "worst-case" interferent compared to other serum proteins such as immunoglobulins or transferrin, which exhibit more limited non-specific uptake in hydrogel matrices [42]. In this context, the observed preferential binding toward the target protein, combined with accurate quantification in untreated serum, supports the conclusion that the imprinted materials exhibit sufficient specificity for operation in complex biological environments.

The binding of BSA to the MIPs (and corresponding NIPs) is shown in Table 1 and Fig. 2, which shows as significant decrease in binding to the MIPs, with 45.5% and 50.0% of the non-target BSA, to the MIP and F-MIP respectively. In contrast, the corresponding non-imprinted control polymers (NIP and F-NIP), exhibited similar binding percentage for non-target BSA, with 47.1% and 50.0% binding (NIP and F-NIP). These results demonstrate that the MIPs are specific and offer excellent selectivity for the chosen target.

Comparing the MIPs against their corresponding NIPs using Eq. 1, allows for the calculation of an imprinting factor (IF), and is a traditional measure of the strength of the interactions of the imprinted polymer towards the template molecule [33]. With this regard, the higher the IF value, the greater the selectivity for the target molecule the MIPs. in the same regard, comparing the binding of the MIP with the target (BHb) vs non-target molecule (BSA), using Eq. 2, produces a selectivity factor (SF) value. The use of a SF value is now generally considered a more favourable method of measuring the performance of a MIP.

$$IF = \frac{\%protein\ rebind\ to\ MIP}{\%protein\ bind\ to\ NIP} \quad (1)$$

$$SF = \frac{\%\ \ target\ protein\ rebind\ to\ MIP}{\%\ \ non-target\ protein\ bind\ to\ MIP} \quad (2)$$

The calculated IF values are presented in Table 2 and show the MIPs have IF values of 2.13 and 2.33 for the MIP and F-MIP, respectively and shows that the MIPs have superior binding performance compared with the corresponding NIPs. These values are above the recommended imprinting threshold of 1.2, used to determine the success of the imprinting effect [19,43]. While the calculated IF value is still an important assessment to showcase the imprinting effect, this has largely been superseded by the uses of a SF value (Table 2), as this allows for an assessment of the MIP's specificity towards the target protein (compared with a non-target protein). The SF values presented in Table 2 show the MIPs have SF values of 1.96 and 1.67 for the MIP and F-MIP, respectively. While there is a drop in values compared with the IF value (especially the F-MIP), these are still above the recommended threshold of 1.2, thus showing good specificity towards the target [19,43].

While the selectivity factors obtained for the imprinted hydrogels are moderate relative to those reported for high optimized antibody systems, it is important to consider these values in the context of practical sensor operation. In complex biological matrices, extreme selectivity often comes at the expense of assay speed, robustness, and matrices tolerance. The hydrogel-based imprinting strategy employed here prioritizes rapid mass transport, high water compatibility, and suppression of non-specific adsorption, enabling reliable quantitative detection directly in serum samples therefore provide a more relevant assessment of sensor performance than selectivity metrics measured under idealized conditions alone.

4.2. Rheological characterisation

For particulate MIP-based sensors intended for suspension assays or flow-assisted detection, mechanical integrity under deformation is a critical yet often overlooked factor influencing signal stability and repeatability. Deformation-induced disruption of the polymer network can alter binding-site geometry, affect target retention, and introduce variability into optical readouts. In this context, rheological characterisation is employed here not as a purely materials-focused investigation, but as a means of elucidating how molecular imprinting influences the

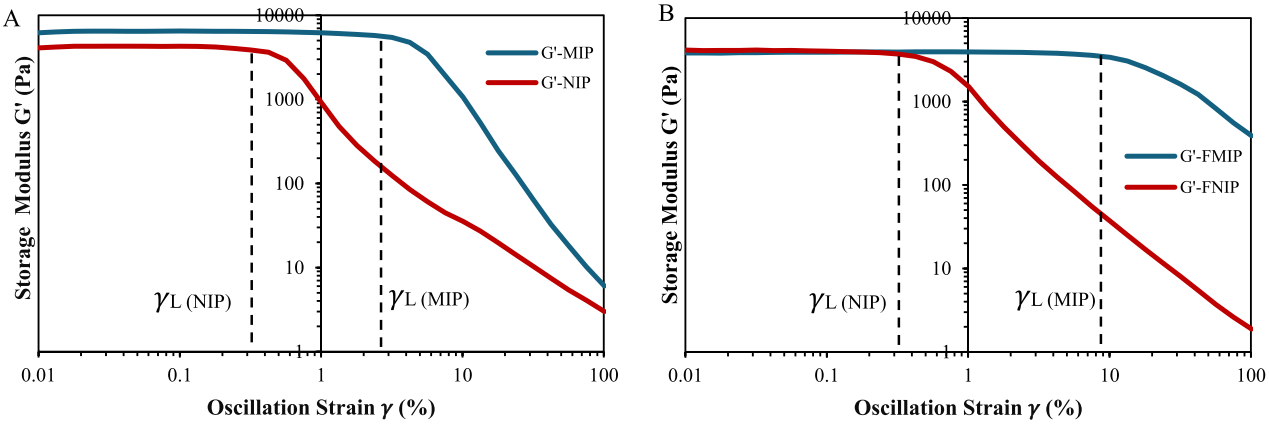

Fig. 3. Strain amplitude sweep test; **A)** MIP (Blue) and **B)** F-MIP (Blue) hydrogel microparticles and their corresponding NIPs (Red) showing the elastic modulus. The verticle dashed line indicates the onset of nonlinear behaviour (γ_L) for each hydrogel, where deviation from the linear viscoelastic region is observed.

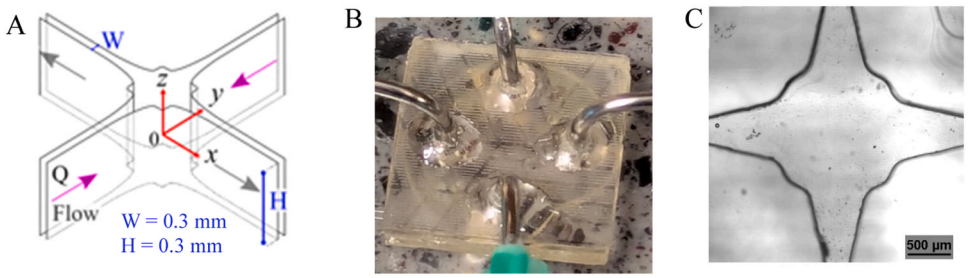

Fig. 4. (**A**) Schematic illustration of the optimised shape cross-slot extension rheometer (OSCER) device, adapted from Calabrese et al., [38] (**B**) Photograph of OSCER 3D printed device assembled and mounted for flow experiments, (**C**) Optical microscopic image of the cross-slot junction region confirming uniform channel dimensions.

mechanical behaviour of the sensing elements under conditions relevant to practical sensor operation.

Whilst MIPs are widely evaluated in terms of binding affinity and selectivity, far less attention has been paid to how imprinting influences the mechanical behaviour of these materials under conditions relevant to chemical sensing and under flow conditions [44–46]. For particulate MIP-based sensors, especially those intended for suspension assays or flow-assisted detection involving repeated handling, mixing and exposure to flow induced stresses, mechanical integrity under deformation and flow is critical to maintaining consistent signal output and binding performance. In this context, rheological characterisation is employed here not as standalone materials studies, but as a tool to elucidate how imprinting alters hydrogel structure in ways that directly impact sensor robustness, target retention, and signal stability, as observed between MIPs and NIPs in the sensing data presented earlier.

Structural integrity was first investigated using strain amplitude sweep tests, presented in Fig. 3. The measurements revealed clear mechanical differences between imprinted and non-imprinted hydrogels. Specifically, the MIPs exhibited a higher linearity limit (γ_L) compared to their corresponding NIPs, indicating enhanced resistence to deformation arising from imprinting-induced network reinforecement (template-bound) [47]. Consistently, the storage modulus (G') of the imprinted hydrogels exceeds that of the NIPs, reflecting a mechanically reinforced polymer network capable of preserving binding-site architecture during sensing operations. This behaviour is consistant with previous reports suggesting that protein occupancy within imprinted cavities can effectively contribute to network stabilisation [48].

Thixotropic recovery experiments further demonstrated the mechanical robustness of the imprinted materials. Following exposure to high strain deformation, the MIPs recovered their original mechanical properties more effectively than the NIPs, supporting their suitability for repeated deformation or/and dynamic flows, as it suggests that imprinting mitigates cumulative structural fatigue and preserves functional performance under conditions commonly encountered in microfluidic and flow-through diagnostic platforms.

When considered alongside the binding and sensing data (Fig. 2 and Tables 1 and 2), the rheological results provide a mechanistic basis for interpreting the observed differences between MIPs and NIPs. Specifically, a mechanically reinforced network with an expanded linear viscoelastic range enables better preservation of cavity geometry during deformation, reducing target loss and signal variability. In this context, the data reinforces the importance of employing a non-template (non-target) protein as a control when assessing MIP (and ultimately sensor) performance, as it more directly probes functional selectivity rather than nominal imprinting efficiency. Consequently, the use of IF as a primary metric for evaluating MIP binding performance – largely inherited form early MIP characterisation frameworks – appears increasingly limited [18].

From a sensing perspective, the enhanced linear viscoelstic range and improved recovery behaviour of the imprinted hydrogels directly support stable fluorescence readout during handling, mixing, and flow-assisted operation. The mechanically reinforced network arising from imprinting-induced structural organization helps preserve binding-site integrity under deformation, thereby reducing signal dirift and variablility. These results demonstrate that the MIP–NIP performance differences reported above arise not solely from chemical recognition, but also from imprinting-induced modifications to the hydrogel network itself, which directly influence mechanical stability and sensing reliability under dynamic conditions. These findings highlight the importance of considering mechanical properties alongside binding affinity when designing MIP-based sensors for real-world applications.

4.3. Molecularly imprinted polymer microparticles under planar extensional flows

Flow-through and microfluidic sensing platforms commonly expose suspended sensing elements to a combination of shear and extensional flow components. While shear-dominated deformation is prevalent along channel walls, extensional and stagnation-point flow fields arise naturally at junctions, contractions, expansions, and mixing regions, where fluid streamlines converge or diverge [49,50]. These extensional components impose sustained stretching and elevated elastic stresses that are qualitatively distinct from simple shear and can be particularly disruptive for soft, swollen polymer networks [51]. For hydrogel-based MIP sensors, such conditions have the potential to alter binding-site accessibility, compromise target retention, and introduce variability into optical readouts. The experiments presented here therefore focus on planar extensional flow as a controlled deformation regime representative of critical regions encountered in practical microfluidic and flow-through sensing environments.

Hydrogel-based MIPs combine molecular selectivity of imprinting the tuneable swelling and mechanical compliance of hydrogel networks, making them attractive candidates for use as responsive sensing elements [52,53]. However, hydrogel materials are known to undergo elastic and viscoelastic deformation under laminar conditions [54], particularly under extensional conditions that generate sustained network stretching and polymer alignment [55]. Although shear-flow exposure is implicitly addressed in many conventional flow-cell and microfluidic sensing formats, controlled planar extensional flow is considerably more difficult to realise experimentally, despite its frequent occurrence in device-relevant geometries. Importantly, extensional deformation represents a stringent “worst-case” mechanical challenge for soft sensing elements, making it especially informative for assessing network robustness and operational reliability. To evaluate the impact of extensional flow on MIP-based sensor performance, a custom 3D-printed optimised shape cross-slot extensional rheometer (OSCER), platform was designed and employed (Fig. 4). The behaviour of intrinsically fluorescent, hydrogel-based MIP microparticles was investigated under stagnation-point flow to assess the stability of template binding and fluorescence signal under deformation conditions relevant to future flow-through and microfluidic chemical sensing applications.

Fig. 4 presents the design, fabrication, and characterisation of the

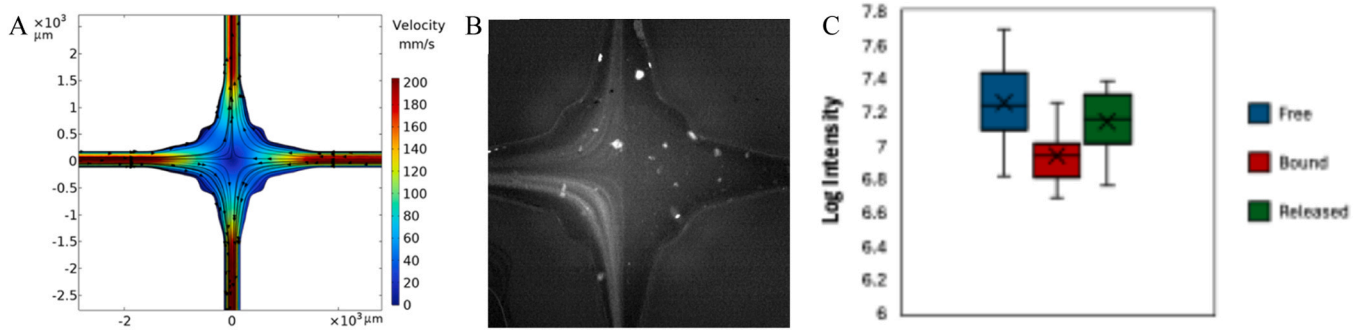

Fig. 5. Behaviour of fluorescently labelled molecularly imprinted polymer (F-MIP) microparticles under planar extensional flow in the OSCER device. (**A**) Representative birefringence image showing the extensional flow field generated at the cross-slot junction, with the stagnation point located at the centre of the device. (**B**) Fluorescence microscopy image of F-MIP microparticles within the junction region under flow, confirming optical visibility and stable interrogation of the sensing elements. (**C**) Logarithmic fluorescence intensity distributions for the free, bound, and released states under extensional flow. Data are shown as mean ± standard deviation (n = 20). The three states remain clearly separated under flow, with low coefficients of variation (CV = 3.21%, 2.09%, and 2.59% for the free, bound, and released states, respectively), demonstrating stable and reversible optical response under deformation.

microfluidic OSCER platform. The cross-junction architecture (Fig. 4 A) consists of orthogonally arranged inlet and outlet channels with precisely defined dimensions (W = 0.3 mm, H = 0.3 mm), enabling controlled laminar flow and reproducible formation of a stagnation point at the channel junction. The assembled 3D-printed device (Fig. 4B) demonstrated reliable fluidic interfacing and optical transparency, allowing real-time optical interrogation of the sensing elements. Microscopic characterisation (Fig. 4 C) confirms accurate reproduction of the designed geometry, with uniform channel dimensions and a well-defined junction region, ensuring predictable flow fields, efficient mass transport, and reproducible sensing performance [38].

Fluid flow through the channels was generated using syringe-driven pumps operating in infusion and withdrawal modes at matched volumetric flow rates, producing stable and well-defined laminar flow conditions. Elevated flow rates were employed to ensure steady velocity profiles and reproducible mass transport, whilst also providing access to high extensional strain rates at the channel junction. These conditions enable systematic evaluation of flow-induced deformation of the hydrogel MIP sensing elements, particularly at the stagnation point where extensional effects are maximised, as illustrated in Fig. 5.

Fig. 5 shows the behaviour of the fluorescently labelled MIP microparticles under planar extensional flow within the OSCER platform. The cross-slot geometry generates a well-defined stagnation point at the channel intersection, where local velocity gradients and extensional strain rates are maximised, providing a controlled deformation regime relevant to demanding microfluidic environments. Fig. 5A illustrates the resulting extensional flow field, while Fig. 5B confirms that the fluorescent MIP microparticles can be stably visualised and interrogated within the junction region under flow.

The corresponding fluorescence response is quantified in Fig. 5C for the free, bound, and released states. To provide a quantitative assessment of sensing performance under deformation, the fluorescence data are presented as logarithmic intensity distributions and analysed as mean ± standard deviation (n = 20). Distinct and reproducible signal levels are observed for all three states, confirming that the fluorescence quenching response remains operational under extensional flow. The calculated coefficients of variation were 3.21%, 2.09%, and 2.59% for the free, bound, and released states, respectively, indicating low signal variability and high reproducibility under dynamic conditions [56,57]. In addition, statistical analysis (two-tailed *t*-test, $p < 0.01$) confirmed that the three fluorescence states are significantly different under flow.

In extensional flow environments, the relevant governing parameter is the local strain rate at the stagnation point rather than bulk flow rate alone, since this determines the degree of hydrogel deformation and the potential perturbation of binding-site geometry. The preservation of distinct fluorescence states with low variability therefore indicates that the imprinted hydrogel network maintains both structural integrity and functional binding capacity during deformation [54,58]. In combination with the rheological results shown in Fig. 3, these findings support the interpretation that molecular imprinting reinforces the hydrogel network, thereby reducing deformation-induced disruption of binding-site geometry and preserving the fluorescence response under extensional flow.

The distinct fluorescence intensity distributions observed for the bound, free, and released states under planar extensional flow confirm that the imprinted hydrogel sensors maintain reversible and quantifiable binding behaviour despite sustained deformation at the stagnation point. This demonstrates that the fluorescence quenching transduction mechanism remains functional under flow-induced stress, an essential requirement for integration into continuous-flow and microfluidic sensor architectures. The results further underscore the importance of evaluating sensing performance under dynamic flow conditions, rather than relying solely on static batch measurements.

4.4. *Molecularly imprinted polymer fluorescent quenching assay*

Incorporation of a covalently bound fluorescent reporter within the imprinted hydrogel matrix enables the MIPs to function directly as optical transducers, converting molecular recognition events into measurable fluorescence signals. In contrast to conventional immunoassays that rely on immobilisation, secondary labels, or enzymatic amplification, the present system exploits intrinsic fluorescence quenching upon target binding to generate a direct and concentration-dependent signal. Fluorescence quenching in the present system arises from binding-induced interactions between the target protein and the embedded fluorophore within the imprinted hydrogel matrix. Upon target recognition, close spatial proximity between the bound protein and the fluorescein moieties promotes predominantly static quenching, associated with ground-state complex formation and local microenvironmental changes (polarity and hydrogen bonding), although contributions from dynamic (collisional) quenching may also occur within the hydrated network [29]. This behaviour can be described by the Stern-Volmer relationship, where the fluorescence intensity decreases as a function of analyte concentration, although deviations from linearity are commonly observed in MIP systems due to heterogenous binding sites and restricted diffusion within polymer matrices [32]. Similar mechanisms have been widely reported in fluorescent MIP-based sensors, where target binding induces localised quenching through proximity effects and perturbation of the fluorophore environment, particularly for protein-fluorophore interactions in polymer scaffolds [59,60]. These effects enable a direct and concentration-dependent optical response that is intrinsically coupled to molecular recognition

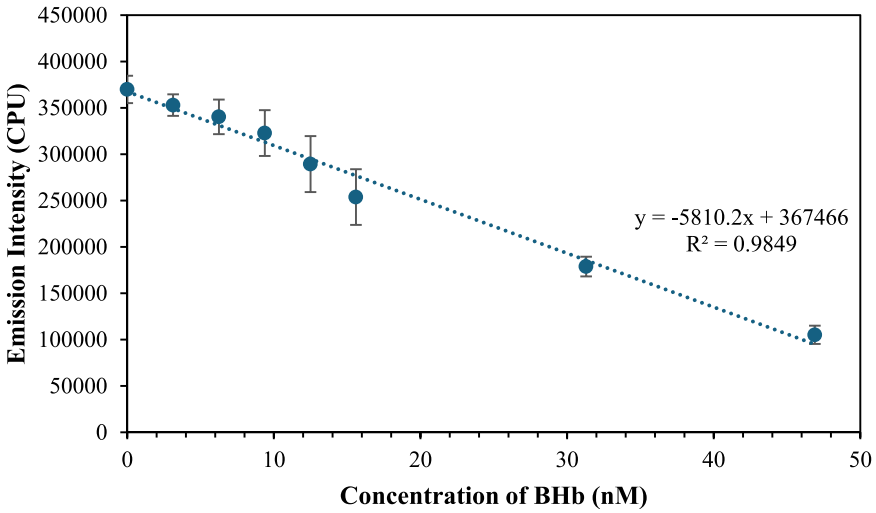

Fig. 6. Calibration plot comparing the amount of protein loaded (mg mL^{-1}) in human serum, with the fluorescence emission intensity (CPS).

within the imprinted cavities. This transduction simplicity reduces assay complexity, minimizes cumulative sources of error, and enables rapid, mix-and measure detection suitable for deployable chemical sensing applications [23].

Initial sensor characterisation was performed using batch rebinding experiments to evaluate the binding behaviour and transduction response of the F-MIPs. The fluorescence quenching data were analysed using kinetic and equilibrium binding isotherms, with the sensor response fitted using a Langmuir adsorption model to extract relevant binding parameters [61,62]. This approach assumes a finite population of effective binding sites and provides a practical framework for describing analyte-sensor interactions in MIP-based sensing systems. Using the binding isotherm presented in Figure S1, the equilibrium dissociation constant (K_D) of the imprinted material was determined to be 1.91 μM. This extracted K_D value is consistent with previously reported affinities for hydrogel-based MIPs and thin-film imprinted gels produced using similar functional monomers, including systems characterised by surface plasmon resonance (SPR) [63]. Importantly, the binding affinity observed here falls within the range typically reported for polyclonal antibodies, highlighting the suitability of the imprinted hydrogel architecture as a synthetic alternative to biological recognition elements in chemical sensing applications [64].

To assess sensor performance in a biological relevant and analytically challenging environment, a competitive assay format was employed using human serum spiked with known concentrations of bovine hemoglobin (BHb). Human serum represents a complex matrix containing a high abundance of potentially interfering species, including albumin, immunoglobulin G (IgG), fibrinogen, and transferrin, making it an appropriate medium for evaluating sensor selectivity and matrix tolerance [40]. The F-MIPs were incubated with the spiked serum samples to allow target association, after which the fluorescence response was measured directly using fluorescence spectroscopy. The ability of the sensor to maintain a quantitative and selective response in serum demonstrates effective suppression of non-specific interactions and confirms the robustness of the F-MIP sensing platform for application in complex biological samples relevant to chemical and biosensing applications

Batch rebinding experiments were performed to characterise the binding behaviour and sensing response of the molecularly imprinted polymers. Equilibrium binding data were analysed using kinetic binding isotherms, with the sensor response fitted using a Langmuir adsorption model to extract relevant affinity parameters. The Langmuir model is expressed as Eq. 3:

Table 3
Amount of target protein (BHb) recovered from a spiked sample.

BHb Spiked Concentration (nM)	Amount of BHb recovered (nM)	Amount of BHb recovered (%)	Percentage Error (%)
8.0	7.8 (± 0.8)	97.5	2.5
14.0	14.1 (± 1.3)	100.7	0.7
23.5	23.2 (	98.7	1.3

$$Q_e = \frac{Q_m C_e}{K_D + C_e} \tag{3}$$

Where Q_e and C_e represent the amount of target protein (BHb) bound per unit mass of MIP an equilibrium BHb concentration, respectively. Q_m denotes the maximum binding capacity of the imprinted material, and K_D is the equilibrium dissociation constant, reflecting the affinity of the imprinted binding sites for the target analyte [61,62].

Sensor calibration was achieved by correlating the loaded BHb concentration (nM) with corresponding fluorescence intensity response (counts per second, CPS), as shown in Fig. 6. From the resulting calibration curve, a limit of detection (LOD) of 8.38 nM and a limit of quantification (LOQ) of 25.39 nM were determined, demonstrating the suitability of the F-MIP sensor for sensitive protein determination in analytically relevant concentration ranges [65].

The analytical performance of the MIP-based fluorescence quenching sensor was further evaluated using human serum samples spiked with known concentrations of target protein (BHb). Three independent samples (1 mL each) were fortified with BHb at concentration of 8.0. 14.0, and 23.5 nM spanning the lower-to-mid region of the sensor's dynamic range. The results of the spike-and recovery experiments are summarised in Table 3.

Across all concentrations tested, the sensor demonstrated excellent analytical accuracy, with recoveries ranging from 97.5% to 100.7% and relative errors below 2.5%. Notably, this level of accuracy was achieved directly in untreated human serum, a complex biological matrix containing high concentrations of potentially interfering proteins such as albumin, immunoglobulins, fibrinogen, and transferrin. The ability of the sensor to maintain quantitative performance under these conditions highlights the effectiveness of the hydrogel-based molecular imprinting strategy in suppressing non-specific adsorption while preserving selective target recognition.

Compared with commercially available antibody-based assays, which often require surface immobilisation, multiple washing steps, and signal amplification to achieve comparable accuracy, the MIP-based

Table 4
A comparison of the developed MIP-based fluorescence sensor with representative antibody-based and synthetic receptor protein assays.

Assay Platform	Recognition Element	Sample Matrix	LOD	Assay Time	Immobilisation
ELISA [66]	Antibody	Serum	nM-μM	2–4 h	Yes
Magnetic Fluorescence Assay [67]	Antibody	Serum	nM range	>1 h	Yes
Fluorescent MIP Sensor [68]	MIP	Buffer	nM range	~30 min	Often
This work	Hydrogel MIP	Serum	8.38 nM	< 10 min	No

assay developed here operates in a simple mix-and measure format while delivering similar or superior analytical precision. This performance advantage can be attributed to the intrinsic selectivity of the imprinted binding sites, combined with the highly hydrated hydrogel matrix that promotes protein accessibility while minimising fouling effects. Furthermore, the direct fluorescence quenching transduction mechanism enables rapid signal generation without the need for enzymatic labels or secondary reagents, reducing assay complexity and cumulative error.

A comparative assessment of the present sensor against representative commercial and literature-report assays is provided in Table 4. The results demonstrate that the developed MIP-based platform achieves competitive sensitivity and accuracy, whilst offering significant practical advantages in terms of assay simplicity, robustness, and compatibility with flow-through and microfluidic sensing formats. Collectively, these findings establish the proposed fluorescence quenching MIP sensor as a high performance and scalable alternative to antibody-based protein assays for chemical and biosensing applications.

Table 4 compares the analytical performance and operational characteristics of the developed hydrogel MIP-based fluorescence sensor with representative antibody-based and synthetic receptor protein assays reported in the literature. As shown, the sensor developed in this work achieves a limit of detection of 8.38 nM directly in human serum, which is comparable to and in some cases superior to, established antibody-based assays, whilst operating with substantially reduced assay time and complexity [23,69]. Conventional immunoassays such as ELISA and magnetic fluorescence assays rely on antibodies as the recognition element and typically require surface immobilisation, multiple incubation and washing steps, and enzymatic or labelled signal amplification [66,67]. While these approaches can achieve high sensitivity, they are inherently time-consuming (often requiring hours), operationally complex, and dependent on the availability and stability of biological recognition elements. In contrast, the MIP-based sensor presented here operates in a rapid (<10 min), mix-and-measure format without immobilisation, workflow while maintaining nanomolar sensitivity in a complex biological matrix.

Compared to previously reported fluorescent MIP sensors, which are often evaluated in buffered solutions and frequently require immobilisation or longer equilibration times, the present system demonstrates a clear advance by achieving quantitative detection directly in serum [70]. This performance highlights the advantages of the hydrogel-based imprinting strategy, which provides a highly hydrated, protein-compatible environment that facilitates rapid mass transport and selective binding while suppressing nonspecific adsorption. The intrinsic fluorescence labelling of the imprinted matrix further enables direct optical transduction, reducing sources of cumulative error associated with multi-step signal generation. Importantly, the use of hydrogel MIPs as synthetic recognition elements offers key benefits from a sensor engineering perspective. MIPs can be produced rapidly, reproducibly, and at low cost, without the need for biological expression systems, cold-chain storage, or batch-to-batch antibody validation. This robustness and scalability make MIP-based sensors particularly attractive for deployment in resource-limited settings, point-of-care diagnostics, and situations where rapid development of assays for emerging biomarkers is required.

The comparison in Table 4 demonstrates that our MIP-based fluorescence sensor combines competitive analytical performance with substantial practical advantages over antibody-based platforms, including reduced assay time, simplified operation, and improved robustness. These attributes position hydrogel MIP sensors as a compelling alternative recognition strategy for next-generation chemical and biosensing applications, particularly in flow-through, microfluidic, and rapid diagnostic formats.

5. Conclusion

In this study, a fluorescence quenching-based protein sensing platform was developed using fluorescently labelled, hydrogel-based molecularly imprinted polymer (MIP) microparticles as synthetic recognition elements. The mild, aqueous imprinting strategy enabled preservation of protein structure during polymerisation, resulting in selective binding cavities with affinity comparable to polyclonal antibodies, whilst offering superior robustness and reproducibility.

The imprinted polymers demonstrated strong selectivity towards hemoglobin, relative to non-imprinted controls and non-target proteins, confirming the effectiveness of the imprinting process. Rheological and microfluidic flow analysis revealed pronounced mechanical differences between imprinted and non-imprinted materials, highlighting the influence of molecular imprinting on polymer network structure and deformation behaviour. These mechanical effects were shown to be directly relevant under both static and planar extensional flow conditions, where preservation of network integrity is essential for maintaining binding-site stability and reliable optical readout in flow-through and microfluidic sensing environments.

Integration of a fluorescent label within the MIP matrix enabled a simple, mix-and-measure fluorescence quenching assay, eliminating the need for surface immobilisation or multi-step signal amplification. The resulting sensor exhibited nanomolar detection limits and high analytical accuracy when applied directly to complex biological media, including human serum, with recovery rates comparable to or exceeding those of commercially available antibody-based assays.

Overall, this work establishes molecularly imprinted hydrogel microparticles as effective active sensing materials for fluorescence-based protein detection. These findings position hydrogel-based molecularly imprinted fluorescence sensors as viable scalable antibody alternatives for next-generation chemical and biosensing applications, particularly in rapid, flow-through, and microfluidic diagnostic formats.

CRediT authorship contribution statement

Federico Sinnona: Investigation. **Sullivan Mark Vincent:** Writing – review & editing, Writing – original draft, Validation, Supervision, Project administration, Methodology, Investigation, Funding acquisition, Formal analysis, Data curation, Conceptualization. **Shen Amy:** Writing – review & editing, Writing – original draft, Supervision, Funding acquisition, Formal analysis, Conceptualization. **Shun Ono:** Investigation. **Abdelgawad Mohamed:** Methodology, Investigation.

Declaration of Competing Interest

The authors declare that they have no known competing financial interests or personal relationships that could have appeared to influence the work reported in this paper.

Acknowledgements

All authors gratefully acknowledge the support of the Okinawa Institute of Science and Technology Graduate University (OIST) with subsidy funding from the Cabinet Office, Government of Japan. The authors would also like to thank the OIST Core Facilities, Imaging Section, for providing access to the SEM and Dr Toshiaki Mochizuki for support.

Appendix A. Supporting information

Supplementary data associated with this article can be found in the online version at doi:10.1016/j.snb.2026.139977.

Data availability

Data will be made available on request.

References

[1] N. Rifai, M.A. Gillette, S.A. Carr, Protein biomarker discovery and validation: the long and uncertain path to clinical utility, Nat. Biotechnol. 24 (2006) 971–983, https://doi.org/10.1038/nbt1235.
[2] K. Strimbu, J.A. Tavel, What are biomarkers? Curr. Opin. HIV Aids. 5 (2010) 463–466, https://doi.org/10.1097/COH.0b013e32833ed177.
[3] R. Mayeux, Biomarkers: potential uses and limitations, NeuroRx 1 (2004) 182–188, https://doi.org/10.1602/neurorx.1.2.182.
[4] V.J.B. Ruigrok, M. Levisson, M.H.M. Eppink, H. Smidt, J. van der Oost, Alternative affinity tools: more attractive than antibodies? Biochem. J. 436 (2011) 1–13, https://doi.org/10.1042/BJ20101860.
[5] V.A. Adhav, K. Saikrishnan, The realm of unconventional noncovalent interactions in proteins: their significance in structure and function, ACS Omega 8 (2023) 22268–22284, https://doi.org/10.1021/acsomega.3c00205.
[6] P. Chames, M. van Regenmortal, E. Weiss, D. Baty, Therapeutic antibodies: successes, limitations and hopes for the future, Br. J. Pharm. 157 (2009) 220–233, https://doi.org/10.1111/j.1476-5381.2009.00190.x.
[7] P.C. Taylor, A.C. Adams, M.M. Hufford, I. de la Torre, K. Winthrop, R.L. Gottlieb, Neutralizing monoclonal antibodies for treatment of COVID-19, Nat. Rev. Immunol. 21 (2021) 382–393, https://doi.org/10.1038/s41577-021-00542-x.
[8] C. Bebbington, G. Yarranton, Antibodies for the treatment of bacterial infections: current experience and future prospects, Curr. Opin. Biotechnol. 19 (2008) 613–619, https://doi.org/10.1016/j.copbio.2008.10.002.
[9] B. Van Dorst, J. Mehta, K. Bekaert, E. Rouah-Martin, W. De Coen, P. Dubruel, R. Blust, J. Robbens, Recent advances in recognition elements of food and environmental biosensors: a review, Biosens. Bioelectron. 26 (2010) 1178–1194, https://doi.org/10.1016/j.bios.2010.07.033.
[10] Committee on Methods of Producing Monoclonal Antibodies Institute for Laboratory Animal Research National, R. C. Monoclonal Antibody Production, National Academy Press, Washington, 1999, https://doi.org/10.17226/9450.
[11] K. Karim, F. Breton, R. Rouillon, E.V. Piletska, A. Guerreiro, I. Chianella, S. A. Piletsky, How to find effective functional monomers for effective molecularly imprinted polymers? Adv. Drug Deliv. Rev. 57 (2005) 1795–1808, https://doi.org/10.1016/j.addr.2005.07.013.
[12] P.A.G. Cormack, A.Z. Elorza, Molecularly imprinted polymers: synthesis and characterisation, J. Chromatogr. B. 804 (2004) 173–182, https://doi.org/10.1016/j.jchromb.2004.02.013.
[13] K. Mosbach, Toward the next generation of molecular imprinting with emphasis on the formation, by direct molding, of compounds with biological activity (Biomimetics), Anal. Chim. Acta 435 (2001) 3–8, https://doi.org/10.1016/S0003-2670(01)00800-5.
[14] A. Leonhardt, K. Mosbach, Enzyme-mimicking polymers exhibiting specific substrate binding and catalytic functions, React. Polym. 6 (1987) 285–290, https://doi.org/10.1016/0167-6989(87)90099-7.
[15] L. Resina, C. Alemán, F.C. Ferreira, T. Esteves, Protein-imprinted polymers: how far have "Plastic Antibodies" come? Biotechnol. Adv. 68 (2023) 108220 https://doi.org/10.1016/j.biotechadv.2023.108220.
[16] H.R. Culver, N.A. Peppas, Protein-imprinted polymers: the shape of things to come? Chem. Mater. 29 (2017) 5753–5761, https://doi.org/10.1021/acs.chemmater.7b01936.
[17] D.R. Kryscio, M.Q. Fleming, N.A. Peppas, Conformational studies of common protein templates in macromolecularly imprinted polymers, Biomed. Micro 14 (2012) 679–687, https://doi.org/10.1007/s10544-012-9648-5.
[18] M.E. Byrne, K. Park, N.A. Peppas, Molecular imprinting with hydrogels, Adv. Drug Deliv. Rev. 54 (2002) 149–161, https://doi.org/10.1016/S0169-409X(01)00246-0.
[19] M. Zayats, A.J. Brenner, P.C. Searson, Protein imprinting in polyacrylamide-based gels, Biomater 35 (2014) 8659–8668, https://doi.org/10.1016/j.biomaterials.2014.05.079.
[20] M.V. Sullivan, S.R. Dennison, G. Archontis, J.M. Hayes, S.M. Reddy, Towards rational design of selective molecularly imprinted polymers (MIPs) for proteins: computational and experimental studies of acrylamide based polymers for myoglobin, J. Phys. Chem. B 123 (2019) 5432–5443, https://doi.org/10.1021/acs.jpcb.9b03091.
[21] G. Selvolini, G. Marrazza, MIP-based sensors: promising new tools for cancer biomarker determination, Sensors 17 (2017) 718, https://doi.org/10.3390/s17040718.
[22] T.S. Bedwell, M.J. Whitcombe, Analytical applications of MIPs in diagnostic assays: future perspectives, Anal. Bioanl. Chem. 408 (2016) 1735–1751, https://doi.org/10.1007/s00216-015-9137-9.
[23] J.W. Lowdon, H. Dilien, P. Singla, M. Peeters, T.J. Cleij, B. Grin, K. Eersels, MIPs for commercial application in low-cost sensors and assays – an overview of the current status Quo, Sens. Actuators B Chem. 325 (2020) 128973, https://doi.org/10.1016/j.snb.2020.128973.
[24] M.M. Kemp, M. Weïwer, A.N. Koehler, Unbiased binding assays for discovering small-molecule probes and drugs, Bioorg. Med. Chem. 20 (6) (2012) 1979–1989, https://doi.org/10.1016/j.bmc.2011.11.071.
[25] O. Tagit, N. Hildebrandt, Fluorescence sensing of circulating diagnostic biomarkers using molecular probes and nanoparticles, ACS Sens 2 (2017) 31–45, https://doi.org/10.1021/acssensors.6b00625.
[26] B. Li, J. Qi, F. Liu, R. Zhao, M. Arabi, A. Ostovan, J. Song, X. Wang, Z. Zhang, L. Chen, Molecular imprinting-based indirect fluorescence detection strategy implemented on paper chip for non-fluorescent microcystin, Nat. Commun. 14 (2023) 6553, https://doi.org/10.1038/s41467-023-42244-z.
[27] T. Takeuchi, T. Mukawa, J. Matsui, M. Higashi, K. Shimizu, Molecular imprinted polymers with matalloporphryin-based molecular recognition sites coassembled with methacrylic acid, Anal. Chem. 73 (2001) 3869–3874, https://doi.org/10.1021/ac010278p.
[28] J. Wang, Y. Wang, H. Qiu, L. Sun, X. Dai, J. Pan, Y. Yan, Y, A novel sensitive luminescence probe microspheres for rapid and efficient detection of τ-fluvalinate in Taihu Lake, Sci. Rep. 7 (2017) 46635, https://doi.org/10.1038/srep46635.
[29] R. Liu, C.C. Ko, Molecularly imprinted polymer-based luminescent chemosensors, Biosensors 13 (2023) 295, https://doi.org/10.3390/bios13020295.
[30] Y. Xu, Y. Zhou, H. Luo, H. Li, T. Ni, G. Xu, O. Sugihara, J. Xie, B. Cai, Molecularly imprinted polymer-coated hybrid optical waveguides for sub-AM fluorescence sensing, Analyst 149 (2024) 800–806, https://doi.org/10.1039/D3AN01008B.
[31] M. Chen, H. Li, X. Xue, F. Tan, L. Ye, Signal amplification in molecular sensing by imprinted polymers, Microchim. Acta 191 (2024) 574, https://doi.org/10.1007/s00604-024-06649-x.
[32] S. Akgönüllü, S. Kılıç, C. Esen, A. Denizli, Molecularly imprinted polymer-based sensors for protein detection, Polymers 15 (2023) 629, https://doi.org/10.3390/polym15030629.
[33] N.W. Turner, C.W. Jeans, K.R. Brain, C.J. Allender, V. Hlady, D.W. Britt, From 3D to 2D: a review of the molecular imprinting of proteins, Biotechnol. Prog. 22 (2006) 1474–1489, https://doi.org/10.1021/bp060122.
[34] T. Bosch-Tamayo, T.M. Iakimova, A.Q. Shen, M.V. Sullivan, Solid-phase engineering of molecularly imprinted nanoparticles (NanoMIPs): how template and solid-phase drive polymer composition and binding performance, J. Mater. Chem. B 13 (2025) 15047–15056, https://doi.org/10.1039/D5TB01580D.
[35] S. Singh, A. Singh, N. Singh, J. Singh, Impedimetric sensing of C-reactive protein using a novel molecularly imprinted polymer coupled with bismuth-enhanced cobalt ferrite nanocomposites for cardiovascular risk assessment, J. Mater. Chem. B 14 (2026) 299–310, https://doi.org/10.1039/D5TB01698C.
[36] S.A. Piletsky, N.W. Turner, P. Laitenberger, Molecularly imprinted polymers in clinical diagnostics—future potential and existing problems, Med. Eng. Phys. 28 (2006) 971–977, https://doi.org/10.1016/j.medengphy.2006.05.004.
[37] C.I. Winder, C. Blackburn, C.L. Hutchinson, A.Q. Shen, N.W. Turner, M.V. Sullivan, Enzyme activity inhibition of α-amylase using molecularly imprinted polymer (MIP) hydrogel microparticles, Biomacromolecules 25 (2024) 7459–7465, https://doi.org/10.1021/acs.biomac.4c01097.
[38] V. Calabrese, A.Q. Shen, S.J. Haward, Naturally derived colloidal rods in microfluidic flows, Biomicrofluidics 17 (2023) 021301, https://doi.org/10.1063/5.0142867.
[39] M.V. Sullivan, S. Nanalal, B.E. Dean, N.W. Turner, Molecularly imprinted polymer hydrogel sheets with metalloporphyrin-incorporated molecular recognition sites for protein capture, Talanta 266 (2024) 125083, https://doi.org/10.1016/j.talanta.2023.125083.
[40] S. Ketrat, D. Japrung, P. Pongprayoon, Exploring how structural and dynamic properties of bovine and canine serum albumins differ from human serum albumin, J. Mol. Graph. Model 98 (2020) 107601, https://doi.org/10.1016/j.jmgm.2020.107601.
[41] J.J. BelBruno, Molecularly imprinted polymers, Chem. Rev. 119 (2019) 94–119, https://doi.org/10.1021/acs.chemrev.8b00171.
[42] Y. He, Z. Lin, Recent advances in protein-imprinted polymers: synthesis, applications and challenges, J. Mater. Chem. B 10 (2022) 6571–6589, https://doi.org/10.1039/D2TB00273F.
[43] E. Verheyen, J.P. Schillemans, M. Van Wijk, M.A. Demeniex, W.E. Hennink, C. F. Van Nostrum, Challenges for the effective molecular imprinting of proteins, Biomaterials 32 (2011) 3008–3020, https://doi.org/10.1016/j.biomaterials.2011.01.007.
[44] M.V. Sullivan, C. Fletcher, R. Armitage, C. Blackburn, N.W. Turner, A rapid synthesis of molecularly imprinted polymer nanoparticles for the extraction of performance enhancing drugs (PIEDs), Nanoscale Adv. 5 (2023) 5352–5360, https://doi.org/10.1039/D3NA00422H.
[45] C. Yu, K. Mosbach, Insights into the origins of binding and the recognition properties of molecular imprinted polymers prepared using an amide as the

hydrogen-bonding functional group, J. Mol. Recognit. 11 (1998) 69–74, https://doi.org/10.1002/(SICI)1099-1352(199812)11:1/6<69::AID-JMR392>3.0.CO;2-I.
[46] K. Mosbach, O. Ramstron, The emerging technique of molecular imprinting and its future impact on biotechnology, Nat. Biotechnol. 14 (1996) 163–170, https://doi.org/10.1038/nbt0296-163.
[47] T. Mezger, The Rheology Handbook, Vincentz Network, 2020, https://doi.org/10.1515/9783748603702.
[48] O. Kimhi, H. Bianco-Peled, Study of the interactions between protein-imprinted hydrogels and their templates, Langmuir 23 (2007) 6329–6335, https://doi.org/10.1021/la700248s.
[49] V. Calabrese, T. Porto Santos, C.G. Lopez, M.P. Lettinga, S.J. Haward, A.Q. Shen, Extensibility governs the flow-induced alignment of polymers and rod-like colloids, Phys. Rev. Res. 6 (2024) L012042, https://doi.org/10.1103/PhysRevResearch.6.L012042.
[50] S.T. Chan, S.J. Haward, A.Q. Shen, Microscopic investigation of vortex breakdown in a dividing T-junction flow, Phys. Rev. Fluids 3 (2018) 072201, https://doi.org/10.1103/PhysRevFluids.3.072201.
[51] V. Calabrese, A.Q. Shen, S.J. Haward, How do polymers stretch in capillary-driven extensional flows? Macromolecules 57 (2024) 9668–9676, https://doi.org/10.1021/acs.macromol.4c01604.
[52] M.V. Sullivan, P. Lasserre, C. Blackburn, N.W. Turner, B. Sellergren, B, Stimuli-responsive molecularly imprinted materials: fundamentals and applications, Responsive Mater. 3 (2025), https://doi.org/10.1002/rpm.20240032.
[53] P. Singla, T. Broughton, M.V. Sullivan, S. Garg, R. Berlinguer-Palmini, P. Gupta, K. J. Smith, B. Gardner, F. Canfarotta, N.W. Turner, E. Velliou, S. Amarnath, M. Peeters, Double imprinted nanoparticles for sequential membrane-to-nuclear drug delivery, Adv. Sci. (2024) e2309976, https://doi.org/10.1002/advs.202309976.
[54] S.J. Haward, Microfluidic extensional rheometry using stagnation point flow, Biomicrofluidics 10 (2016) 043401, https://doi.org/10.1063/1.4945604.
[55] D.N. Ku, Blood flow in arteries, Annu. Rev. Fluid Mech. 29 (1997) 399–434, https://doi.org/10.1146/annurev.fluid.29.1.399.
[56] D.A. Armbruster, T. Pry, Limit of Blank, limit of detection and limit of quantitation, Clin. Biochem. Rev. 29 (2008) S49–S52.
[57] A. Shrivastava, V. Gupta, Methods for the determination of limit of detection and limit of quantitation of the analytical methods, Chron. Young-.-. Sci. 2 (2011) 21, https://doi.org/10.4103/2229-5186.79345.
[58] V. Calabrese, S. Varchanis, S.J. Haward, J. Tsamopoulos, A.Q. Shen, Structure-property relationship of a soft colloidal glass in simple and mixed flows, J. Colloid Interface Sci. 601 (2021) 454–466, https://doi.org/10.1016/j.jcis.2021.05.103.
[59] Y. Shao, X. Rong, H. Zhao, H. Feng, W. Ma, W. Peng, G. Gao, X. Yang, Z. Jiao, Fluorescent molecularly imprinted polymer sensor prepared using mesoporous silica as carrier for selective detection of bisphenol A, Microchim. Acta 193 (2026) 245, https://doi.org/10.1007/s00604-026-07947-2.
[60] L. Zeng, X. Zhang, X. Wang, D. Cheng, R. Li, B. Han, M. Wu, Z. Zhuang, A. Ren, Y. Zhou, T. Jing, Simultaneous fluorescence determination of bisphenol A and its halogenated analogs based on a molecularly imprinted paper-based analytical device and a segment detection strategy, Biosens. Bioelectron. 180 (2021) 113106, https://doi.org/10.1016/j.bios.2021.113106.
[61] Patiha, E. Heraldy, Y. Hidayat, M. Firdaus, The langmuir isotherm adsorption equation: the monolayer approach, IOP Conf. Ser. Mater. Sci. Eng. 107 (2016) 012067, https://doi.org/10.1088/1757-899X/107/1/012067.
[62] D.B. Finlay, S.B. Duffull, M. Glass, 100 years of modelling ligand–receptor binding and response: a focus on GPCRs, Br. J. Pharm. 177 (2020) 1472–1484, https://doi.org/10.1111/bph.14988.
[63] H.F. El-Sharif, N.W. Turner, S.M. Reddy, M.V. Sullivan, Application of thymine-based nucleobase-modified acrylamide as a functional Co-monomer in electropolymerised thin-film molecularly imprinted polymer (MIP) for selective protein (Haemoglobin) binding, Talanta 240 (2022) 123158, https://doi.org/10.1016/j.talanta.2021.123158.
[64] R.R. Mustafa, R. Sukor, S.M. Mohd Nor, N. Saari, F.M. Kamal, A.Z. Mohsin, Enhancement of binding affinity of anti-hapten polyclonal IgG recognizing mitragynine using affinity purification, Pertanika J. Sci. Technol. 29 (2021) 2451, https://doi.org/10.47836/pjst.29.4.11.
[65] A.D. McNaught, A. Wilkinson, Limit of Detection. The IUPAC Compendium of Chemical Terminology, fifth ed., International Union of Pure and Applied Chemistry, NC, 2025 https://doi.org/10.1351/goldbook.L03540.
[66] RayBiotech. Human Hemoglobin ELISA Kit. ⟨https://www.raybiotech.com/human-hemoglobin-elisa-elh-hgb?gad_source=1&gbraid=0AAAAD_Bj67JqLMJrGgOcojBzHx014amI&gclid=Cj0KCQjwvpy5BhDTARIsAHSilynEkMGxLDTBLIG3QfMxBcH6Y0dkDe8GWMMeXsW3JnrznouPUPVR-SIaAhfVEALw_wcB⟩, 2025 (accessed 12 December 2025).
[67] Biocompare. Hemoglobin (HB) Magnetic Fluorescence Assay. ⟨https://www.biocompare.com/25138-Assay-Kit/21536477-Hemoglobin-HB-Magnetic-Fluorescence-Assay-Kit/⟩, 2025 (accessed 12 December 2025).
[68] Chondrex. Hemoglobin Assay kit. ⟨https://www.chondrex.com/products/hemoglobin-assay-kit⟩, 2025 (accessed 12 December 2025).
[69] D. Kim, A.E. Herr, Protein immobilization techniques for microfluidic assays, Biomicrofluidics 7 (2013) 41501, https://doi.org/10.1063/1.4816934.
[70] A. Elbelazi, F. Canfarotta, J. Czulak, M.J. Whitcombe, S. Piletsky, E. Piletska, Development of a homogenous assay based on fluorescent imprinted nanoparticles for analysis of nitroaromatic compounds, Nano Res. 12 (2019) 3044–3050, https://doi.org/10.1007/s12274-019-2550-1.

Federico Sinnona is a PhD candidate in Bioengineering and Medical-Surgical Sciences at Politecnico di Torino, Italy, where he is affiliated with the Department of Mechanical and Aerospace Engineering (DIMEAS). He holds a master's degree in biomedical engineering from Politecnico di Torino, during which he developed a 3D in vitro spinal cord model. His research experience includes a research fellowship at the Okinawa Institute of Science and Technology, focusing on smart substrates for protein biomarker detection. His current doctoral research is centered on integrating smart biomaterials, advanced biofabrication techniques such as 3D bioprinting and organ-on-chip technologies, and biomimetic hydrogels to develop physiologically relevant in vitro kidney models for studies in physiology, disease mechanisms, and pharmacological screening.

Mohamed Shoieb Abdelgawad is a Postdoctoral Researcher in the Datta Lab at the California Institute of Technology, where he investigates the fluid mechanics of complex solutions and their instabilities to enhance transport, mixing, and microscale processes. He earned his PhD from the Okinawa Institute of Science and Technology Graduate University (OIST) in Japan, where his work focused on the elastic behaviour and rheology of yield stress fluids in diverse flow configurations including microchannels. His research interests bridge fluid dynamics, polymer physics, and microfluidic transport phenomena relevant to chemical sensing and actuation systems.

Shun Ono is a PhD student at the Okinawa Institute of Science and Technology Graduate University (OIST), Japan, where he is engaged in research on laboratory automation systems and microfluidic devices for biological experimentation. He received his Bachelor of Science in Biology from the University of Tokyo, where his undergraduate research focused on developing molecular detection systems using solid-state nanopores. His current work at OIST involves leveraging microfluidics to advance automated and high-precision biological assays relevant to sensing and actuation in chemical and bioengineering applications.

Prof. Amy Q. Shen is Provost and a Professor in the Micro/Bio/Nanofluidics Unit at the Okinawa Institute of Science and Technology Graduate University (OIST), Japan, where she leads research on microfluidics, complex fluid mechanics, and lab-on-a-chip technologies at bio-nano interfaces with applications in biosensing and chemical analysis. She received her Ph.D. in Theoretical and Applied Mechanics from the University of Illinois at Urbana-Champaign and held faculty positions at Washington University in St. Louis and the University of Washington before joining OIST. Her interdisciplinary work combines experiments, theory, and modelling to investigate rheology, non-Newtonian flows, and microfluidic transport phenomena, and to develop innovative micro- and nanofluidic platforms for sensing and diagnostics. She is a Fellow of the American Physical Society, the Royal Society of Chemistry, and the Society of Rheology, and serves on editorial boards of several journals in fluid mechanics, microfluidics, and soft matter.

Dr. Mark V. Sullivan is a senior researcher in the Micro/Bio/Nanofluidics Unit at the Okinawa Institute of Science and Technology Graduate University (OIST), Japan. He earned his PhD in Molecularly Imprinted Polymers from the University of Central Lancashire (UK) in 2019, followed by postdoctoral research at De Montfort University and the University of Sheffield, where he developed aptamer-molecularly imprinted nanoparticle hybrids and other synthetic recognition materials. At OIST, his research focuses on creating novel recognition materials as alternatives to antibodies for biosensing and diagnostic applications, including integration with microfluidic platforms for real-time chemical detection. His interdisciplinary work bridges polymer chemistry, materials science, and microscale sensing technologies.